Journal of Rehabilitation in Civil Engineering 9-1 (2021) 84-101

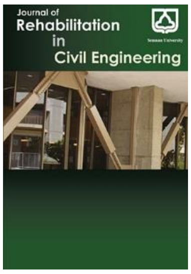

journal homepage: http://civiljournal.semnan.ac.ir/

Investigation of Earthquake Significant Duration on the Seismic Performance of Adjacent Steel Structures in Near-Source

M. Rezaee Manesh[1], S. Fattahi[1] and H. Saffari[2*]

1. Master of Science in Earthquake engineering, Water and Environment Engineering Faculty Shahid Beheshti University, Tehran, Iran

2. Assistant Professor, Faculty of Civil, Water and Environmental Engineering, Shahid Beheshti University, Tehran, Iran

Corresponding author: *h_saffari@mail.sbu.ac.ir*

ARTICLE INFO

Article history:
Received: 10 May 2020
Accepted: 05 October 2020

Keywords:
Significant Duration,
Impact of Buildings,
Seismic Joint,
Near Fault Area.

ABSTRACT

According to the recent Earthquake records, the earthquake duration is longer in some areas, resulting into more structural damage. One of the important factors in reducing earthquake damages is the separation gap between two adjacent structures. This case study investigated the effect of significant duration of the earthquake on two adjacent steel moment-resisting structures with different heights and near to active fault. The pounding between pairs of three 3, 6 and 9-story steel moment frames was evaluated using a nonlinear time history analysis method considering the reduced stiffness and strength. The results showed that for the intended type 3-soil, the risk of pounding and collapse amplification among the 3- and 6-story buildings are higher than others. This is due to the necessity of the Iranian standard 2800 to calculate the separation gap by the nonlinear methods for the buildings with height more than 8 stories. Also, the analysis of the significant duration of the applied earthquakes demonstrated that this parameter is a determining and effective factor in the pounding of structures, especially the adjacent buildings with different heights. It is noteworthy all of the analysis was done by 9 earthquake records. This study recommended using the nonlinear method to calculate separation gap while designing two adjacent steel moment-resisting structures with different heights in the near-field area and on the soft soil.

1. Introduction

The duration of earthquake ground motion has a significant effect on the degree of structural damage. Many physical processes such as decrees in stiffness and strength level in any structures depend on the number of load/ stress cycles occurring during the earthquake. A short-duration motion, though having a large amplitude, may not generate a sufficient number of load cycles resulting in structural collapse. On the other hand, a motion with medium amplitude but a long duration will create

DOI: 10.22075/JRCE.2020.20373.1410

sufficient load cycles to cause damage to the structures. The ground motions with high magnitude and intensity and the recorded reports of far places from the epicenter, all confirm the long duration of earthquakes. Therefore, the structures built in these areas should have more load-bearing capacity, considering the conditions of the site soil [1].

Earthquake duration is directly related to the seismic magnitude [2]. Several researchers have studied the relationship between the structural damage and the duration of earthquake ground motion. Chai et al. (1998) suggested that a long duration ground motion increases the non-elastic design base shear [3]. Despite various studies to examine the specifications of the earthquake ground motion duration and the existence of several different definitions of duration, there is still a need for further study on this issue. Seismic design regulations paid little attention to predicting equations of duration compared to the damping equations for spectral accelerations. Past studies have examined the effect of earthquake duration on the seismic response and emerge of liquefaction (e.g. [4,5]).

Chandramohan et al. (2016) showed the collapse capacity of a modern steel moment frame and a reinforced concrete bridge pier using the sets of spectrally equivalent short- and long-duration records. They found out by sensitivity analyses of the structural model parameters that the structures with high deformation capacities and rapid rates of cyclic deterioration show the greatest sensitivity to the duration [6]. However, nowadays, various methods have been proposed to consider the reduction of stiffness and strength. For instance, Capraro (2018) investigated the impact of subduction motions on the design, particularly the effect of duration, and evaluated the damage potential of them [7]. Fairhurst et al. (2019) investigated the effect of earthquake duration on the design and collapse risk of reinforced concrete shear wall buildings from 6 to 30 stories. Both design and collapse levels of shaking were considered through nonlinear incremental dynamic analysis [8].

Chandramohan (2016) surveyed the influence of structural collapse risk and the integration in the design and assessment practices. The broad objective of this study was to evaluate the influence of ground motion duration on the structural collapse risk, and it was found to be significant to propose methods to consider for the performance assessment and design of structures [9]. Abbaszadeh Shahri et al. (2013) provided an improved method for seismic site characterization with an emphasis on the liquefaction phenomenon [10]. In the case of structural seismic demand, the findings depend on the considered parameters. On the other hand, the studies that only perform peak deformations or peak inter-story changes have not reported a clear correlation with the duration (e.g., [11,12]). On the other hand, the studies have shown the effect of duration on the global response measures (e.g [13,14]), depending on the cumulative response indicators, such as energy loss or a number of non-elastic cycles. However, in general, the seismic codes do not allocate the ground motion duration. New studies on the assessment of overturning capacity have revived the interest in the effects of duration (e.g, [15–17]).

The relationship between the duration and the maximum amplitude of earthquake ground motions is important for the seismic design of structures, especially reinforced concrete structures, which suffer from stiffness and reduced strength in successive earthquake cycles [18].

Robert Jankowski and Sayed Mahmoud (2016) studied about adjacent three-story buildings Linking to reduce structural pounding in the earthquake. Their study results demonstrate that the use of the additional link elements does not change the response of the stiffer and heavier building. The final result of their research shows that linking two buildings allows us to reduce the in-between gap size substantially while structural pounding can be still prevented [19]. Barbosa et al. (2017) estimated the effect of earthquake ground motion duration on the damage in the steel moment-resisting frames. They presented an analytical study on the effect of the ground motion duration on the structural damage of 3-, 9- and 20-story steel moment frame buildings [17]. Bravo-Haro et al. (2018) examined the effect of earthquake duration on the response of steel moment frames [20]. Hoseini Vaez and Tabaei Aghdaei (2019) investigated the effect of the frequency content of the earthquake on damage detection in steel frames [21].

Eftychia A. Mavronicola et al. (2020) investigated the effect of ground motion pounding of base-isolated buildings seismic response against adjusting structures [22]. Zengin et al. (2020) examined the effect of ground motion duration on the structural damage and overturning of steel structures and concluded that the maximum inter-story drift ratio is generally not sensitive to the difference in duration between short-term and long-term records, while the cumulative damage parameters (i.e., dissipated hysteretic energy and modified Park–Ang damage index) of the buildings considered in this study were affected by the duration [23]. Naeej et al. (2019) studied the stochastic analysis of adjacent structures subjected to structural pounding under earthquake excitation [24].

The investigations into the collapse of structures show that in some cases, the lack of sufficient distance between the structures has been reported to be the main cause of the damage. Pounding occurs due to the out-of-phase vibration of adjacent structures that have not sufficient spacing. The damage caused by the pounding of structures has been observed in the earthquakes of Tokachi-Oki in Japan (1968), Managua (1972), Alaska (1964), Friuli in Italy (1976), Romania (1977), Greece (1978, 1981, 1986), Mexico City (1985), Loma Prieta (1989), Northridge (1994), Kobe (1995) and Izmir in Turkey (2001). In the 1989 Loma Prieta earthquake, the pounding phenomenon was directly involved in a wide range of damages observed in structures [25].

In the 1985 Mexico City earthquake, more than 15% of the 330 buildings that suffered serious structural damage or were completely destroyed were caused by the pounding phenomenon [26].

Barros et al. (2013) investigated the influence of seismic pounding on RC buildings with and without base isolation system subject to near-fault ground motions. Focusing on the numerical investigation, they studied the effectiveness of impact and energy dissipation. They suggested a new impact model with three springs and dashpot [27], In the seismic design regulations of different countries, to prevent the pounding of two adjacent structures, a separation gap is suggested as the minimum distance. The fourth edition of Iranian Standard No. 2800 [28] also briefly describes this issue and considers only the height factor as the main variable, so that linear and nonlinear relations are presented according to the number of building floors for the separation gap. Chau et al. (2004) studied the pounding between two adjacent three-story buildings with the same floor height through the multi-degree of freedom elastoplastic concentrated-mass models with the nonlinear viscoelastic pounding model. The results showed that the pounding has a greater effect on the behavior of lighter and more ductile building and increases the responses. In other words, the behavior of heavier and stiffer building had a lower effect than pounding [29].

Anagnostopoulos et al. (1992) extended the studies on the single-degree-of-freedom systems to the multi-degree-of-freedom systems. They also examined the linear and nonlinear responses of several adjacent buildings in a row under the pounding conditions. They idealized the structures as a concentrated mass with a bilinear force-displacement relation and viscoelastic supports, as shown in Figure (1). The stiffness coefficient of the springs was determined by considering the mat foundation on the hard soil. The poundings were simulated by the viscoelastic pounding element with the application of five real earthquakes and the damping constant for the contact element was considered to be 0.5 [30].

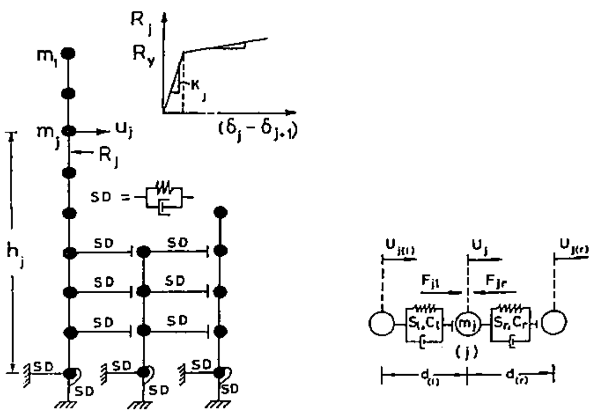

Fig. 1. Modeling of adjacent buildings [30].

They found that pounding may increase the stresses, especially when the colliding buildings have fundamental differences in mass, height, and period [30].

The paper is organized as follows: section 2 presents criteria of different regulations for the separation gap, section 3 presents study methodology, section 4 investigates analysis of pounding between structures and conclusions are drawn in Section 5. This study aims to highlight the importance of earthquake significant duration on the impact of steel structures near-fault zone on soft soil. Results showed that for the mentioned soil type, the risk of pounding and collapse amplification among the 3- and 6-story buildings is higher than in other cases. Also, the analysis of significant duration of the applied earthquakes showed that this parameter is a determining and effective factor in the pounding of structures, especially the adjacent buildings with the height difference, and should be considered in the structural design.

1.1. Types of Seismic Duration

There are different methods for determining the duration of ground motions using the effective characteristics and parameters of the earthquake acceleration-time curve. The methods that define the duration of ground motions using the characteristics of recorded accelerograms of earthquakes can be divided into three categories as follows.

1.1.1. Bracketed Duration

Bracketed duration is the simplest definition of duration where the time interval between the first and last time the acceleration of the ground motion exceeds a certain value is considered as the earthquake duration. In this regard, Page [31] considered the earthquake duration based on the acceleration threshold as 0.05 g. Figure (2) shows an accelerometer, squared acceleration diagram, and process of calculating the bracketed duration with the absolute acceleration limit of 0.05g [32].

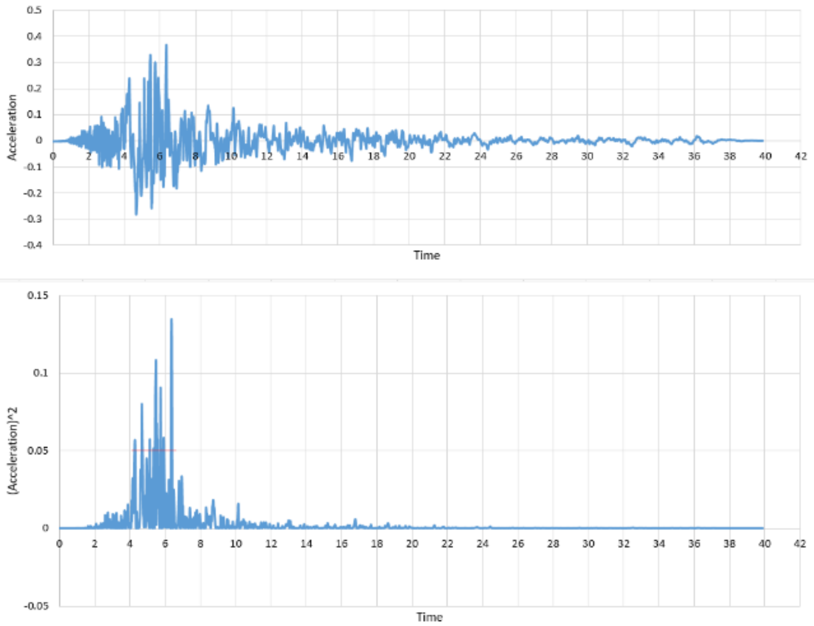

Fig. 2. Calculation process for the bracketed duration with acceleration limit of 0.05g for Loma Prieta earthquake [32].

1.1.2. Uniform Duration

Uniform duration is another definition that takes the overall characteristics of a record into account. This duration is the sum of the time intervals where acceleration exceeds a certain value. Bolt [33] proposed this definition with two threshold values: 0.05g and 0.10g. Figure (3) shows an accelerometer, squared acceleration diagram, and process of calculating the uniform duration with the absolute acceleration limit of 0.1g [32].

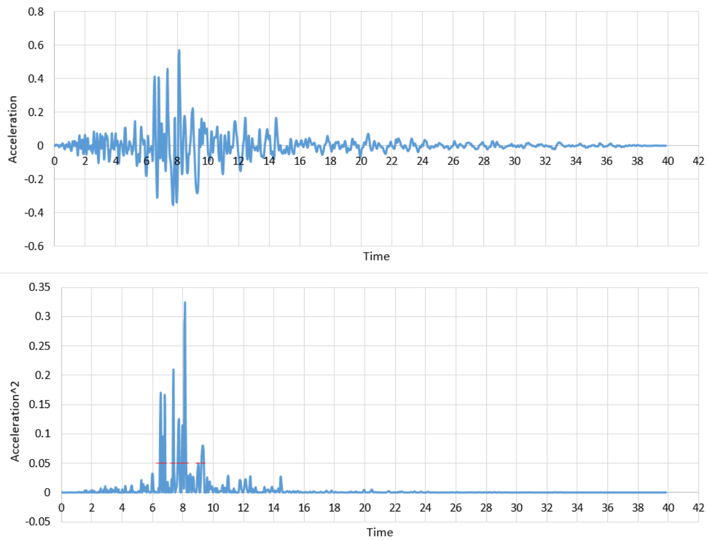

Fig. 3. Calculation process for the uniform duration with acceleration limit of 0.05g for Northridge earthquake [32].

Maximum uniform duration is always less than bracketed duration and is limited to approximately one-fifth of the corresponding bracketed duration [34].

1.1.3. Significant Duration

The third category of definitions is based on the cumulative distribution of earthquake energy, which is determined using the accelerogram. This definition is called the significant duration. The significant duration is calculated based on the integration of the squared ground acceleration. The Arias intensity is used in most of the definitions, which is expressed by the following relation [35]:

$$I_A = \frac{\pi}{2g}\int_0^T a^2(t)dt \qquad (1)\ [35]$$

In this equation, a(t) is the acceleration at time t, which is determined by the accelerogram record. T is the duration of the total strong ground motion and I_A represents the amount of energy applied to the structure.

$D_{s(5-95\%)}$ significant duration 5-95%: the time interval at which 5-95% of $\int_0^{tmax} a(t)^2dt$ is accumulated [36].

$D_{s(5-75\%)}$ significant duration 5-75%: the time interval at which 5-75% of $\int_0^{tmax} a(t)^2dt$ is accumulated [37].

Figure 4.(a) shows the time history of ground motion acceleration recorded at the CIGO station of the 2002 Denali earthquake and Figure 4.(b) shows the standard Arias intensity cumulative curve of the record. The $D_{s(5-75\%)}$ of the record in Figure 4.(a) is 27.67s [38].

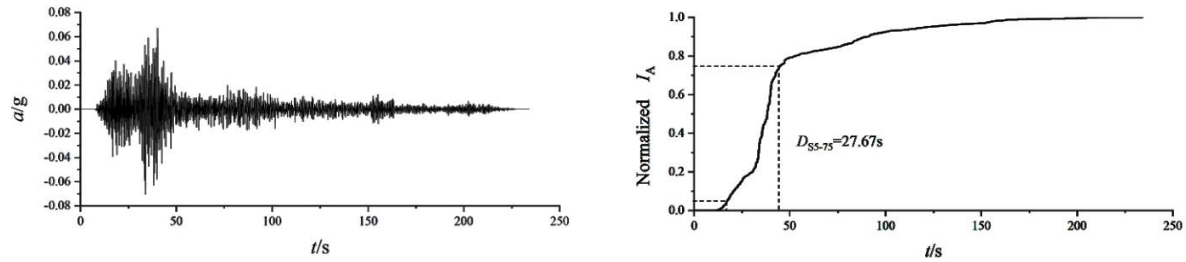

(a) acceleration time history (b) significant duration $D_{s(5-75\%)}$

Fig. 4. Acceleration time history and significant duration $D_{s(5-75\%)}$ of ground motion [38].

Understanding the effect of ground motion duration on the cumulative damage and failure mechanism will bring us one step closer to preventing the earthquake-induced collapse in the near future and can also help improve the building regulations.

In this study, the effect of significant duration of the earthquake on two adjacent steel moment structures with different heights was investigated. The pounding between pairs of three 3-, 6- and 9-story steel moment frames was evaluated using the nonlinear time history analysis considering the reduced stiffness and strength. The results of pounding and the effect of collapse amplification were shown by comparing the number and level of formed hinges and the options of collapse amplification were discussed.

1.2. Building Performance Levels

Building performance levels are used to determine the purpose of improvement. The level of performance of the building indicates the vulnerability of structural and non-structural components [39]. Building performance levels are as follows:

- **I**mmediate **O**ccupancy (IO)
- **L**ife **S**afety (LS)
- **C**ollapse **P**revention (CP)

2. Criteria of Different Regulations for Separation Gap

Several solutions have been proposed by engineers to reduce the lateral displacement and prevent the pounding of buildings due to seismic motions. In fact, the first and simplest way to reduce the pounding force is to create enough space between two buildings. All the authentic regulations in the world have dealt with this issue, and each one has proposed a distance to create a safe space between two buildings. In the seismic design regulations of different countries, a separation gap has been suggested as the minimum distance to prevent the pounding of two adjacent structures. Table 1 summarizes these criteria.

Table 1. Criteria of regulations for the separation gap [28].

Row	Regulation	separation gap calculation formula
1	Iranian Regulation No. 2800	$\Delta_{MT}= \sqrt{(\Delta_{M1})^2 + (\Delta_{M2})^2}$
2	UBC97	$S_i = \sqrt{(\Delta_{i1})^2 + (\Delta_{i2})^2}$
3	FEMA 273	$\delta_{MT} = \sqrt{(\delta_{M1})^2 + (\delta_{M2})^2}$
4	ASCE_SEI_7_16	$\delta_{MT} = \sqrt{(\delta_{M1})^2 + (\delta_{M2})^2}$
5	Eurocode8	$d_s = q_d d_e$

In Table 1, Δ_{M1} and Δ_{M2} are the displacement of two adjacent structures. Δ_{i1} is the lateral displacement of the structure at the ith level relative to the ground level and Δ_{i2} is the lateral displacement of the adjacent building at the ith level relative to the ground level, both of which must be calculated according to the criteria of this regulation. δ_{M1} and δ_{M2} are maximum nonlinear lateral displacement of structures. d_s is the displacement of a point of the structure under the seismic analysis, q_d is a factor of displacement response modification, and d_e is the displacement obtained from the same point of the structure by the spectral analysis.

3. Methodology

In this case study 3, 6 and 9-story buildings; as a representative of low-rise, mid-rise and high-rise structures respectively; were modeled to explore the effect of duration on the pounding of adjacent steel buildings with different heights. The height criterion for introducing the low-, mid- and high-rise structures in Table 2 was obtained from the Hazus' [40] guideline.

Table 2. Classification of high-, mid- and low-rise structures based on height [40].

Number Range of	Label/Description	Height Name	Stories
1	Wood Frame	All	All
2	Steel Frame	Low-Rise	1-3
3		Mid-Rise	4-7
4		High-Rise	8 and up
5	Concrete Frame	Low-Rise	1-3
6		Mid-Rise	4-7
7		High-Rise	8 and up
8	Masonry	Low-Rise	1-3
9		Mid-Rise	4-7
10		High-Rise	8 and up
11	Manufactured Housing		All

First, the optimal sections were designed by Etabs software, then, SeismoStruct and it's models of stiffness and strength degradation were used for accurate analysis .However, the aim is to compare these models in different elevation arrangements, and our goal of optimal design is to bring the conditions of the structures closer to reality. Using Etabs 2015 software, three-dimensional (3D) modeling of steel structures was performed. The site soil was considered as type III according to Standard 2800, which refers to an area of high seismic risk. Structures were designed by dynamic analysis of nonlinear time history technique. Member design and loading were based on the tenth and sixth issues of the national building regulations respectively. Table 3 shows the load specifications.

Table 3. Loading specifications.

Row	Load type	Loading level	values	Unite
1	dead	stories	520	Kg/m2
2	dead	roof	500	Kg/m2
3	live	stories	200	Kg/m2
4	live	roof	200	Kg/m2

All structures had 4 span in x and y directions. The height of the floors was 3 m and the length of the span was 4 m. The buildings were regular in terms of the plan and height. The lateral load-bearing system was assumed to be the intermediate moment frame in both directions and the floor diaphragm to be rigid on its plane. The section of the columns and beams was box and I-shaped plate girder respectively. Once the optimum sections were designed, a two-dimensional (2D) frame of each structural model was selected, modeled and controlled again using Siesmostruct2019. The optimum sections properties are shown in Table 4 and Figure 5.

Table 4. Optimum sections of columns and beams of steel floor structures.

Elevation code	Column dimensions (cm)	Beam dimensions (cm)	Column dimensions (cm)	Beam dimensions (cm)	Column dimensions (cm)	Beam dimensions (cm)
	3-story steel structure		6-story steel structure		9-story steel structure	
1st floor	$Box_{20\times20\times1.8}$	$B_{w20\times1.5-f15\times1.5}$	$Box_{30\times30\times1.5}$	$B_{w25\times1.5-f20\times1.5}$	$Box_{45\times45\times2}$	$B_{30\times1.5-30\times1.5}$
2nd floor	$Box_{20\times20\times1.3}$	$B_{w20\times1.5-f15\times1.5}$	$Box_{30\times30\times1.3}$	middle $B_{w25\times1.5-f20\times1.5}$ beside $B_{w25\times1.8-f20\times1.8}$	$Box_{40\times40\times1}$	$B_{30\times1.5-30\times1.5}$
3rd floor	$Box_{20\times20\times1}$	$B_{w20\times1-f15\times1}$	$Box_{30\times30\times1}$	middle $B_{w25\times1.5-f20\times1.5}$ beside $B_{w25\times1.8-f20\times1.8}$	$Box_{40\times40\times1}$	$B_{30\times1.8-25\times1.8}$
4th floor			$Box_{25\times25\times1.3}$	$B_{w25\times1.5-f20\times1.5}$	$Box_{30\times30\times1.5}$	$B_{30\times1.5-25\times1.5}$
5th floor			$Box_{20\times20\times1.3}$	middle $B_{w20\times1.5-f15\times1.5}$ beside $B_{w25\times1.3-f20\times1.3}$	$Box_{30\times30\times1.5}$	$B_{30\times1.5-25\times1.5}$
6th floor			$Box_{20\times20\times1}$	$B_{w20\times1-f15\times1}$	$Box_{30\times30\times1}$	$B_{25\times1.8-20\times1.8}$
7thfloor					$Box_{30\times30\times1}$	$B_{25\times1.5-20\times1.5}$
8th floor					$Box_{20\times20\times1.3}$	$B_{20\times1.5-15\times1.5}$
9th floor					$Box_{20\times20\times1}$	$B_{20\times1-15\times1}$

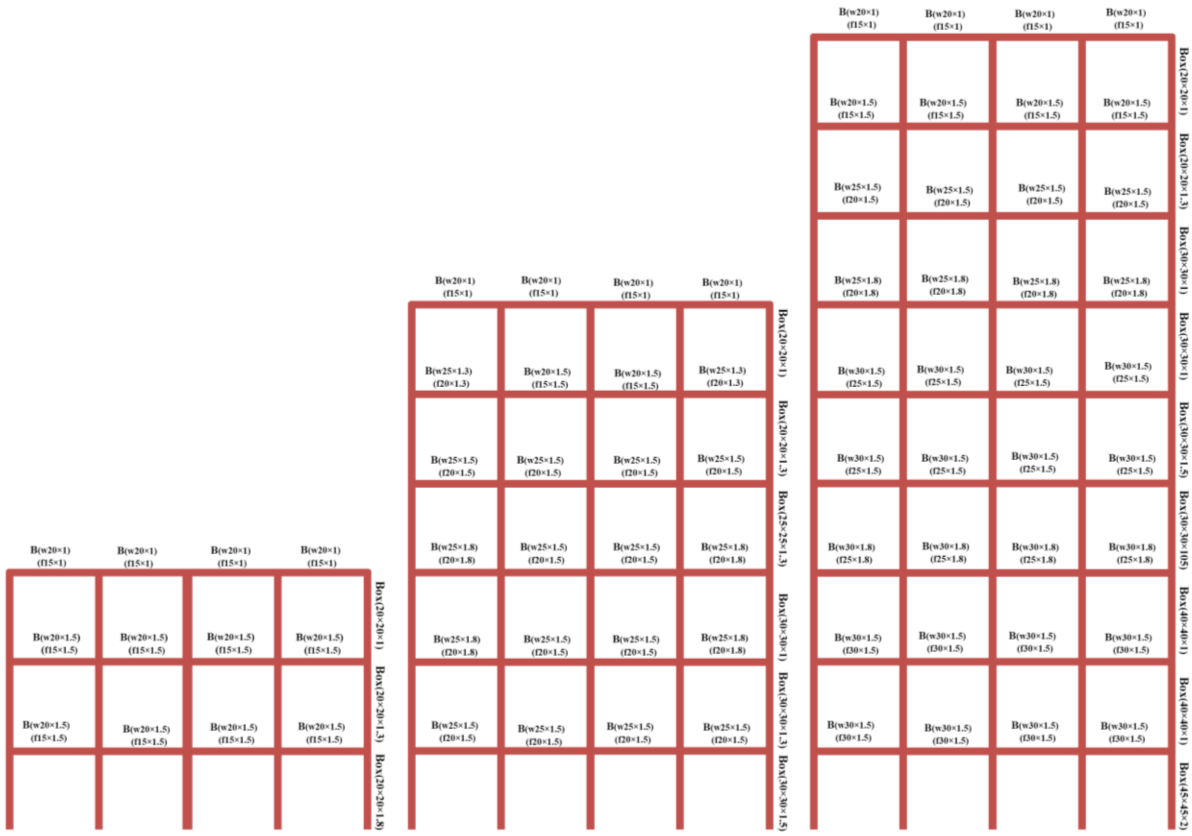

Fig. 5. Section properties graphically.

The amount of allowable plastic flexural deformation for beams and columns and also the desired coefficients to define joint performance levels was obtained according to the tables and criteria of FEMA 356 [36] and then applied in Seismostruct2019. As mentioned earlier, this study aimed to investigate the pounding effect of the structures located on the type III soil. Therefore, structural analysis was performed in the previous step under the circumstances of the type III soil spectrum. After designing and obtaining the optimum sections of the structures, the loading and specifications of the middle frame of each structure were selected, and once again, they were modeled in pairs with the middle frame of other structures in Seismostruct 2019. The frames were put together without any distance. The Gap compression element was used to simulate the pounding. The behavior of this element (shown in Figure 6) is such that it has a nonlinear nature with a bilinear stiffness. In this way, the stiffness of this element is active only when the two structures are in contact with each other, and the stiffness of the element is considered to be zero if the structures are separated from each other. Two general features are used as inputs to introduce the Gap compression element into the software. The first feature is the linear behavior, which includes linear stiffness and linear damping coefficients for the connection element which was considered to be zero in order to prevent from the effect of linear properties of Gaps in vibration modes of the structure. The second one is the nonlinear properties of the element including the span, which determines the compression domain and nonlinear stiffness of the element [41].

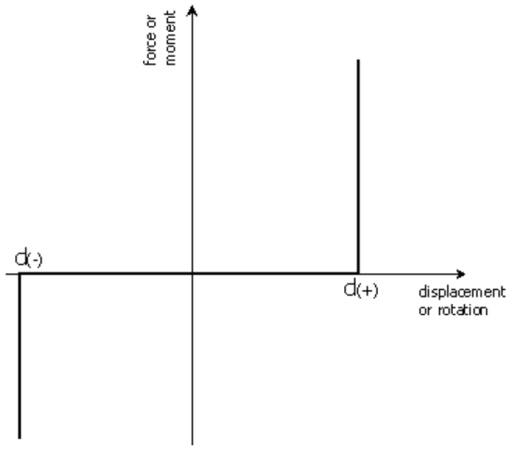

Fig. 6. The curve employed to model structural gapping/pounding, expansion joints, deck restrainers, and so on [42].

The span of this element is considered equal to the separation gap of the structures, and according to the Standard 2800, the separation gap for the structures with eight stories and less is 0.005h (structure height), and for the structures with more than eight stories, it is determined using the design nonlinear lateral displacement. This contact element is used in all places where there is a possibility of pounding between two structures, namely the entire height of the shorter building at the pounding level of the floors. The position of steel frames adjacent to each other (analytical models) is shown in Figure 7.

Fig. 7. Steel frames adjacent to each other (analytical models).

Regarding the validation of the performed analyses, it is noted that all the analyses performed with this software were done under an academic and registered license, and the outputs are far from possible errors related to not using the original version of other software. Also, a comparison of the analyses with Sap, Etabs and Perform3D software analyses shows relative matching of the outputs, but due to the advanced SeismoStruct software in terms of considering the effects of stiffness and strength reduction on different models, it was used in the final analysis. In this study, nine accelerograms were used. All records were obtained from the PEER Strong Motion Database website [43].

There are several key points to consider when selecting the records. First, the significant duration of 5-95% of the accelerograms was considered from short-term to long-term values (5.1 to 15.1 seconds) to be examined in the results. Second, the type of the records site, in other words, shear wave velocity over the uppermost 30 m is similar to the shear wave velocity in the type III soils, namely 175 m/s $<V_{s30}<$375 m/s, according to the classification of Standard 2800. Third, the moment magnitude of the records is between 6.06 and 7.62, and the reverse or reverse strike-slip mechanism is observed in the records, and the records are related to the near-field area fault (at most 11.09 km). The peak ground acceleration of the records ranges from 0.6g to 0.8g. The selected records were used without any modification and scaling to examine the actual behavior of the structure exhibiting during a possible earthquake. Table 5 shows the specifications of the selected records.

Table 5. selected records.

Row	Significant Duration (5-95)% (s)	Arias Intensity (m/s)	Event	Year	Station	Moment Magnitude	PGA (g)	Fault Mechanism	Rrup (km)	Vs30 (m/s)
1	7	5.7	Gazli, USSR	1976	Karakyr	6.8	0.70	Reverse	5.46	259.59
2	9.1	4.1	Coalinga-01	1983	Pleasant Valley P.P. - yard	6.36	0.60	Reverse	8.41	257.38
3	5.2	2	N. Palm Springs	1986	North Palm Springs	6.06	0.69	Reverse Oblique	4.04	344.67
4	12.5	5.3	Northridge-01	1994	Jensen Filter Plant Administrative Building	6.69	0.61	Reverse	5.43	373.07
5	15.1	6	Northridge-01	1994	Sylmar - Converter Sta	6.69	0.62	Reverse	5.35	251.24
6	7.5	3.9	Chuetsu-oki, Japan	2007	Kashiwazaki City Center	6.8	0.65	Reverse	11.09	394.38
7	12.7	5.8	Chi-Chi, Taiwan	1999	TCU065	7.62	0.78	Reverse Oblique	0.57	305.85
8	5.1	5.2	Chi-Chi, Taiwan-06	1999	TCU079	6.3	0.77	Reverse	10.05	363.99
9	6.3	5.2	Niigata, Japan	2004	NIG019	6.63	0.80	Reverse	9.88	372.33
Max	15.1					7.62	0.80		11.09	373.07
Min	5.1					6.3	0.70		0.57	251.24

In order to investigate the effect of pounding on the nonlinear response of buildings, in the first step, all models were subjected to the dynamic analysis of nonlinear time history using the accelerograms through two different states: 1) individually, 2) the frames adjacent to each other, under the nine accelerograms, and in the next step results corresponding to the plastic hinges of the structural members were extracted and compared with each other in both cases. Finally, the effect of the earthquakes with the significant duration of 5-95% was investigated and the results were obtained.

4. Analysis of Pounding between Structures

In this section, the pounding between pairs of 3-, 6- and 9-story structures under nine records with different durations was evaluated using the nonlinear time history analysis. Then, based on the curve of the forces created in the Gaps, it was determined whether the pounding occurred or not. The number of plastic hinges in the structures by applying the separation gap of Standard 2800 and the number of hinges formed in individual structures (in other words by applying sufficient separation gap) were compared with each other. Tables 6 to 8 show the number of hinges before and after the pounding if accrued. Figure 9 shows the analysis results for the pounding of two 3- and 6-story structures under the record NO.4 and the formation of plastic hinges in the IO and LS performance level before and after the pounding as an example.

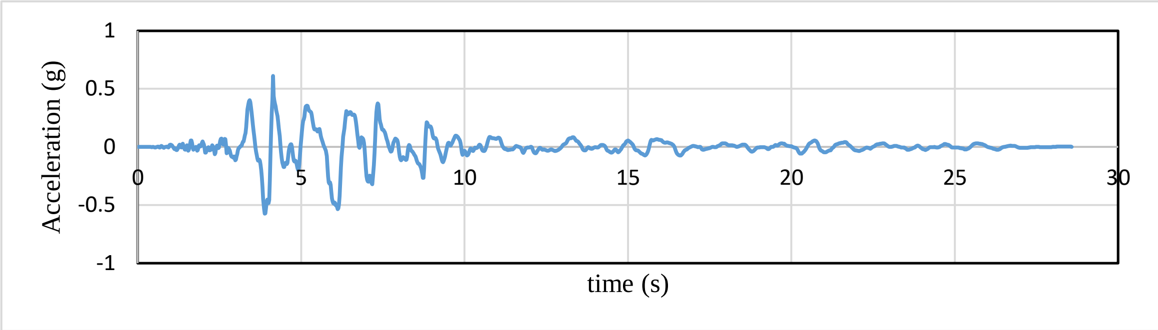

a) Earthquake Record No. 4 (Jensen Filter Plant Administrative Building).

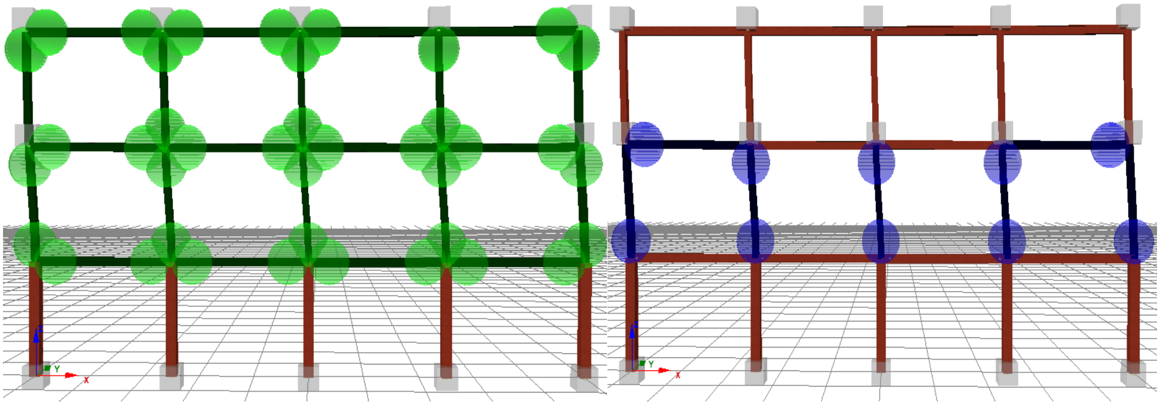

b) IO (green) and LS (blue) hinges of the 3-story structure before pounding.

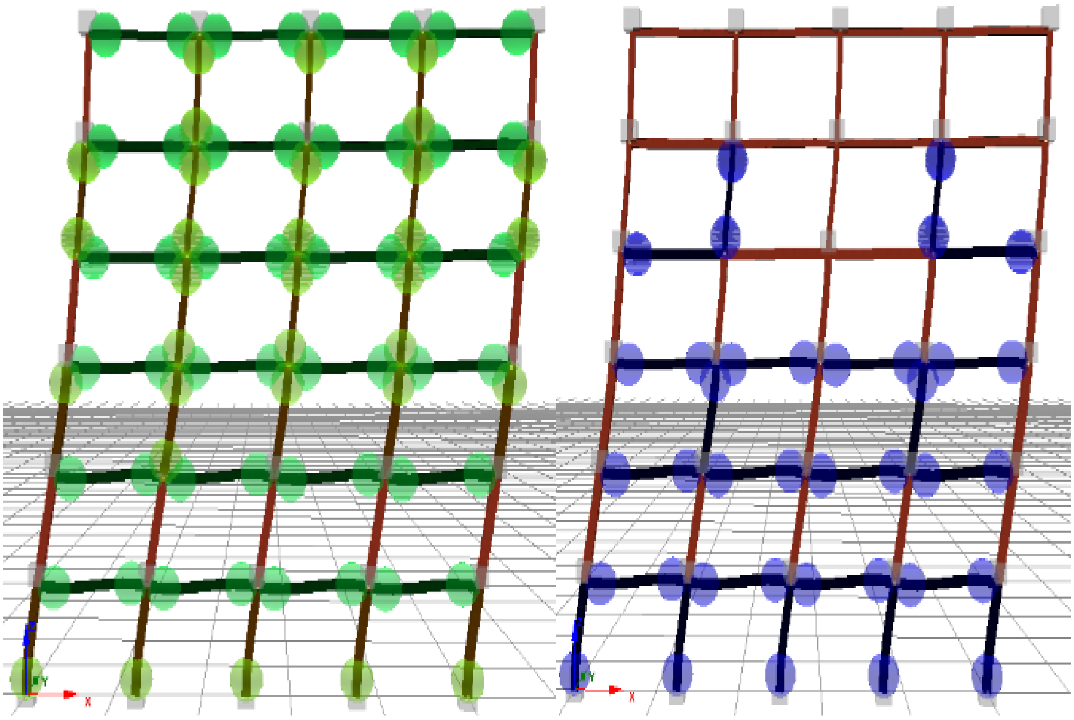

c) IO (green) and LS (blue) hinges of the 6-story structure before pounding.

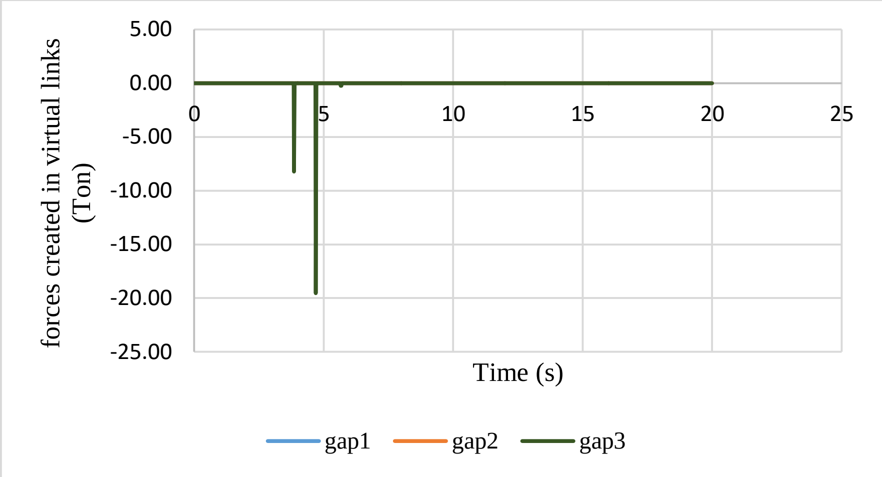

d) Diagram of forces created in virtual links of pounding in 3- and 6-story structure.

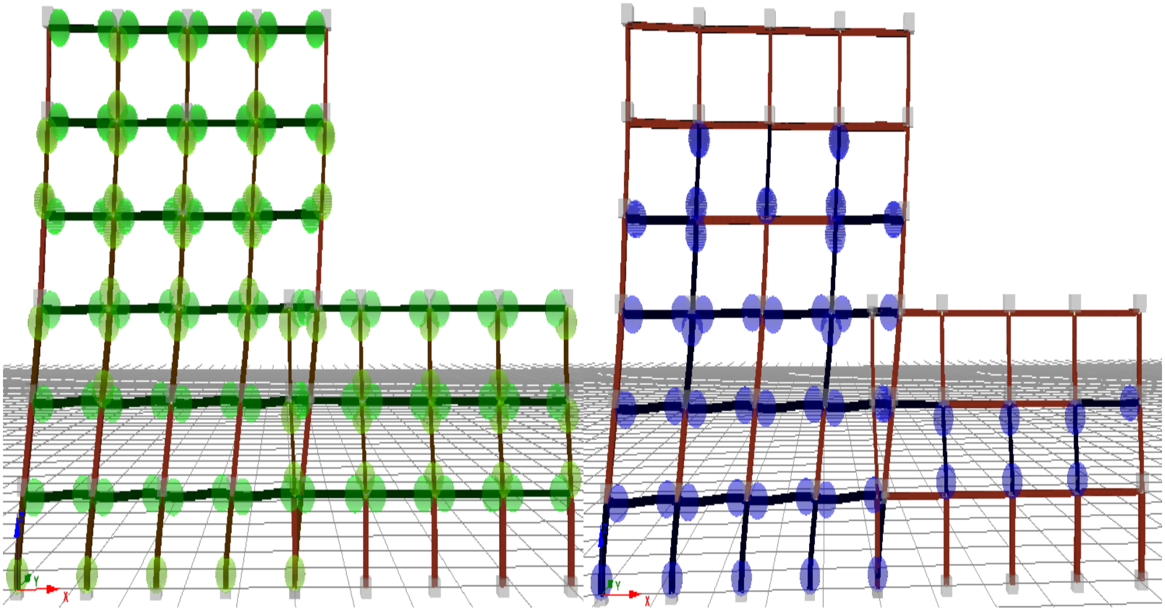

e) Plastic hinges of IO(green) and LS(blue) performance level formed in 3- and 6-story frames.

Fig. 8. Results of pounding analysis in two 3- and 6-story structures under record 4 (Jensen Filter Plant Administrative Building).

Figure 8 (a) shows Earthquake Record No.4 and 8 (b) and (c) show the plastic hinges of the IO and LS performance level formed in the 3- and 6-story frames with sufficient separation gap respectively (without pounding). The diagram of the forces created in the virtual links of pounding in the 3- and 6-story structures in Figure 8 (d), which indicates the pounding of two structures when applying the separation gap of Standard No. 2800. The force created in gap 3 is much greater than the two others. Because the collision was in the roof area, the force of gap1 and gap 2 is very small and zero. Figure 8 (e) shows the plastic hinges of the IO and LS performance levels formed in the 3- and 6-story frames after the collision. By comparing the joints before and after the collision, it was understood that the number of LS joints in 6-story was increased and acted as a fuse, reducing the LS joints of the three-story structure. It should be noted that the entanglement of the two structures after the pounding is due to the magnification settings in the Seismostruct software.

Table 6. Comparison of hinges before and after pounding (3- and 6-story buildings).

Performance levels	Steel Frames	Record 1		Record 2		Record 3		Record 4	
		Joints with sufficient Seismic Joint	Joints (by applying standard Seismic JointNo.2800)	Joints with sufficient Seismic Joint	Joints (by applying standard Seismic JointNo.2800)	Joints with sufficient Seismic Joint	Joints (by applying standard Seismic JointNo.2800)	Joints with sufficient Seismic Joint	Joints (by applying standard Seismic JointNo.2800)
IO	3-Story	37	38	37	38	35	35	40	40
	6-Story	74	76	73	73	73	73	80	81
LS	3-Story	2	-	-	-	-	-	10	7
	6-Story	-	-	6	6	-	-	37	41
CP	3-Story	-	-	-	-	-	-	8	7
	6-Story	-	-	4	4	-	-	24	25

Table 6. Comparison of hinges before and after pounding (3- and 6-story buildings) (Continue).

Performance levels	Steel Frames	Record 5		Record 6		Record 7	
		Joints with sufficient Seismic Joint	Joints (by applying standard Seismic JointNo.2800)	Joints with sufficient Seismic Joint	Joints (by applying standard Seismic JointNo.2800)	Joints with sufficient Seismic Joint	Joints (by applying standard Seismic JointNo.2800)
IO	3-Story	42	40	37	38	37	39
	6-Story	76	78	73	72	76	81
LS	3-Story	10	3	2	2	2	1
	6-Story	16	24	15	14	20	36
CP	3-Story	8	-	-	-	-	-
	6-Story	5	3	-	-	15	10

Table 7. Comparison of hinges before and after pounding (6- and 9-story buildings).

Performance levels	Steel Frames	Record 4	
		Joints with sufficient Seismic Joint	**Joints (by applying standard Seismic Joint No.2800)**
IO	6-Story	80	80
	9-Story	103	123
LS	6-Story	37	38
	9-Story	29	30
CP	6-Story	24	24
	9-Story	17	17

Table 8. Comparison of hinges before and after pounding (3- and 9-story buildings).

Performance levels	Steel Frames	Record 5	
		Joints with sufficient Seismic Joint	Joints (by applying standard Seismic Joint No.2800)(
IO	3-Story	42	42
	9-Story	98	99
LS	3-Story	10	9
	9-Story	2	2
CP	3-Story	8	7
	9-Story	-	-

As shown in the tables 6-8:

- The 3- and 6-story steel structures collided under 7 records from 9 records.
- The 6- and 9-story structures collided under record 4.
- The 3- and 9-story structures collided under record 5.

The 3- and 6-story structures collided under all 6 records, while the 6- and 9-story structures collided only under record 4, and the 3- and 9-story structures collided only under record 5. According to Table 4, which contains the specifications of the records, the highest significant duration of 5-95% is related to both records 4 and 5, which shows the sensitivity of the structures with high height difference to the significant duration.

Record 1 has the highest PGA value (equal to 0.7g) and records 4 and 5 have PGA of 0.61g and 0.62g, respectively, but the significant duration of 5-95% in record 1 is equal to 7 seconds and in records 4 and 5 is 12.5 and 15.1 seconds, respectively. The 6- and 9-story and the 3- and 9-story structures collided in records 4 and 5 also. This indicates that the significant duration of 5-95% is a determining and effective factor in the pounding of structures and should be studied in the design.

5. Conclusion

In this study, according to the results of the studies presented in the introduction and the literature review by the authors of this paper, among the various concrete, steel and masonry structures with different lateral load-resisting systems, the steel moment structure was selected. This type of building has the highest lateral displacement during the earthquake compared to other mentioned buildings. On the other hand, due to the architectural considerations and the presence of large openings along the width of the building, this system is one of the most commonly used types of buildings implemented in Iran. On the other hand, the type of the site soil was selected in a range of dense to moderate including many amplification effects. Then, the pounding between pairs of 3-, 6- and 9-story steel frames was selected in terms of reduced stiffness and strength (in successive loading cycles) and was evaluated using the nonlinear time history analysis. Different records were selected based on different durations, all with the peak ground acceleration from 0.6g to 0.8g, soil type III (dense to moderate soil) as per earthquake regulations No. 2800, $175 < V_{S30} < 375$, moment magnitude between 6.06 and 7.62, reverse fault mechanism, and epicentral distance less than 12 km (near-field area). Therefore the records with the same conditions were considered, and the comparison of the damage severity (increase in the number and levels of plastic hinges in the case with and without pounding) was performed on different durations. The results showed that the 3- and 6-story steel frames had the highest pounding among the selected records. On the other hand, changing the criteria of the Iranian regulations No. 2800 in the high-rise buildings (more than eight stories), which necessitates the use of nonlinear displacement by performing the nonlinear analysis, has created a safety margin and difference in the results of the pounding analysis, which causes the pounding of the 9-story structure with the 3- and 6-story structures only in the records that have a high duration. Therefore, it is concluded that the significant duration is a determining and effective factor in the pounding of adjacent structures with the height difference and should be studied in the structural design. It is also recommended to use the nonlinear relations of the Iranian Standard No. 2800 to calculate the separation gap in the near-field areas on the type III soil for the adjacent steel buildings with a moment-resisting system and the difference in the height.

As a suggestion for future research, IDA analysis can be used to examine the effect of earthquake significant duration on the seismic performance of adjacent structures., and also more exact and better results will be obtained if more records be used in the analysis.

REFERENCES

[1] Raghunandan M. Influence of long duration ground shaking on collapse of reinforced concrete structures. University of Colorado at Boulder, 2013.

[2] Salmon MW, Short SA, Kennedy RP. Strong motion duration and earthquake magnitude relationships. Lawrence Livermore National Lab., CA (United States); EQE International, In; 1992.

[3] Chai YH, Fajfar P, Romstad KM. Formulation of Duration-Dependent Inelastic Seismic Design Spectrum. J Struct Eng 1998;124:913–21. doi:10.1061/(ASCE)0733-9445(1998)124:8(913).

[4] Verdugo R, González J. Liquefaction-induced ground damages during the 2010 Chile earthquake. Soil Dyn Earthq Eng 2015;79:280–95. doi:10.1016/j.soildyn.2015.04.016.

[5] Bhattacharya S, Hyodo M, Goda K, Tazoh T, Taylor CA. Liquefaction of soil in the Tokyo Bay area from the 2011 Tohoku (Japan) earthquake. Soil Dyn Earthq Eng 2011;31:1618–28. doi:10.1016/j.soildyn.2011.06.006.

[6] Chandramohan R, Baker JW, Deierlein GG. Quantifying the Influence of Ground Motion Duration on Structural Collapse Capacity Using Spectrally Equivalent Records. Earthq Spectra 2016;32:927–50. doi:10.1193/122813eqs298mr2.

[7] Capraro I. Damage, collapse potential and long duration effects of subduction ground motions on structural systems. University of British Columbia, 2018.

[8] Fairhurst M, Bebamzadeh A, Ventura CE. Effect of Ground Motion Duration on Reinforced Concrete Shear Wall Buildings. Earthq Spectra 2019;35:311–31. doi:10.1193/101117EQS201M.

[9] Chandramohan R. Duration of earthquake ground motion: Influence on structural collapse risk and integration in design and assessment practice. 2016.

[10] Abbaszadeh Shahri A, Rajablou R, Ghaderi A. An Improved Method for Seismic Site Characterization with Emphasis on Liquefaction Phenomenon. J Rehabil Civ Eng 2013;1:53–65.

[11] CA C. Does duration really matter? Proceedings of the FHWA/NCEER workshop on the national representation of seismic ground motion for new and existing highway. Burlingame, California: Organized by NCEER project 106-F-5.4.1 and ATC project ATC-18-1 facilities. 1997.

[12] Iervolino I, Manfredi G, Cosenza E. Ground motion duration effects on nonlinear seismic response. Earthq Eng Struct Dyn 2006;35:21–38. doi:10.1002/eqe.529.

[13] Hancock J, Bommer JJ. A State-of-Knowledge Review of the Influence of Strong-Motion Duration on Structural Damage. Earthq Spectra 2006;22:827–45. doi:10.1193/1.2220576.

[14] Dutta A, Mander JB. Energy Based Methodology for Ductile Design of Concrete Columns. J Struct Eng 2001;127:1374–81. doi:10.1061/(ASCE)0733-9445(2001)127:12(1374).

[15] Bommer JJ, Magenes G, Hancock J, Penazzo P. The Influence of Strong-Motion Duration on the Seismic Response of Masonry Structures. Bull Earthq Eng 2004;2:1–26. doi:10.1023/B:BEEE.0000038948.95616.bf.

[16] Raghunandan M, Liel AB. Effect of ground motion duration on earthquake-induced structural collapse. Struct Saf 2013;41:119–33. doi:10.1016/j.strusafe.2012.12.002.

[17] Barbosa AR, Ribeiro FLA, Neves LAC. Influence of earthquake ground-motion duration on damage estimation: application to steel moment resisting frames. Earthq Eng Struct Dyn 2017;46:27–49. doi:10.1002/eqe.2769.

[18] Rezaee Manesh M, Saffari H. Relationships Between Significant, Bracketed and Uniform Durations with Earthquake Indices and Site Conditions Using Iranian Seismic Data. Sharif Journal of Civil Engineering. 2021 doi:10.24200/j30.2020.55728.2769

[19] Jankowski R, Mahmoud S. Linking of adjacent three-storey buildings for mitigation of structural pounding during earthquakes. Bull Earthq Eng 2016;14:3075–97. doi:10.1007/s10518-016-9946-z.

[20] Bravo-Haro MA, Elghazouli AY. Influence of earthquake duration on the response of steel moment frames. Soil Dyn Earthq Eng 2018;115:634–51. doi:10.1016/j.soildyn.2018.08.027.

[21] Hoseini Vaez SR, Tabaei Aghdaei SS. Effect of the frequency content of earthquake excitation on damage detection in steel frames. J Rehabil Civ Eng 2019;7:124–40.

[22] Mavronicola EA, Polycarpou PC, Komodromos P. Effect of ground motion directionality on the seismic response of base isolated buildings pounding against adjacent structures. Eng Struct 2020;207:110202. doi:10.1016/j.engstruct.2020.110202.

[23] Zengin E, Abrahamson NA, Kunnath S. Isolating the effect of ground-motion duration on structural damage and collapse of steel frame buildings. Earthq Spectra 2020;36:718–40. doi:10.1177/8755293019891720.

[24] Naeej M, Vaseghi Amiri J, Jalali SG. Stochastic Analysis of Adjacent Structures Subjected to Structural Pounding under Earthquake Excitation. J Rehabil Civ Eng 2019;7:153–65.

[25] Pantelides CP, Ma X. Linear and nonlinear pounding of structural systems. Comput Struct 1998;66:79–92. doi:10.1016/S0045-7949(97)00045-X.

[26] Maison BF, Kasai K. Analysis for a Type of Structural Pounding. J Struct Eng 1990;116:957–77. doi:10.1061/(ASCE)0733-9445(1990)116:4(957).

[27] Barros RC, Naderpour H, Khatami SM, Mortezaei A. Influence of seismic pounding on RC buildings with and without base isolation system subject to near-fault ground motions. J Rehabil Civ Eng 2013;1:39–52.

[28] Earthquake Design Building Regulations (Standard 2800). (1385) Third Edition, Road, Housing & Urban Development Research Center, n.d.

[29] Chau KT, Wei XX, Shen CY, Wang LX. Experimental and theoretical simulations of seismic torsional poundings between two adjacent structures. 13th World

Conf. Earthq. Eng. 13WCEE, 2004, p. 1–6.

[30] Anagnostopoulos SA, Spiliopoulos K V. An investigation of earthquake induced pounding between adjacent buildings. Earthq Eng Struct Dyn 1992;21:289–302. doi:10.1002/eqe.4290210402.

[31] Page RA. Ground motion values for use in the seismic design of the trans-Alaska pipeline system. vol. 672. US Geological Survey; 1972.

[32] Rezaee Manesh M, Saffari H. Empirical equations for the prediction of the bracketed and uniform duration of earthquake ground motion using the Iran database. Soil Dyn Earthq Eng 2020;137:106306. doi:10.1016/j.soildyn.2020.106306.

[33] Bolt BA. Duration of strong ground motion. Proc. 5th World Conf. Earthq. Eng., vol. 1, 1973, p. 1304–13.

[34] Rezaee Manesh M, Saffari H, Analytical study of seismic durability and its destructive effects on structures and distribution of accelerated seismic durability of Iran, Disaster Prevention and Management Knowledge, vol 0. 3. 253-266

[35] Arias A. A measure of earthquake intensity in: Seismic Design for Nuclear Power Plants, Hansen, RJ 1970.

[36] Trifunac MD, Brady AG. A study on the duration of strong earthquake ground motion. Bull Seismol Soc Am 1975;65:581–626.

[37] Chandramohan R, Baker JW, Deierlein GG. Quantifying the Influence of Ground Motion Duration on Structural Collapse Capacity Using Spectrally Equivalent Records. Earthq Spectra 2016;32:927–50. doi:10.1193/122813EQS298MR2.

[38] Lingfeng K, Maosheng G, Zhanxuan Z. The effect of duration of strong ground motion on the ductility demand of SDOF structure. IOP Conf Ser Earth Environ Sci 2019;304:032079. doi:10.1088/1755-1315/304/3/032079.

[39] FEMA 356 Prestandard and Commentary for the Seismic Rehabilitation of Buildings, American Society of Civil Engineers. November 2000.

[40] Security D of H, Agency FEM, Division M, Washington DC. Hazus-MH, Multi-hazard Loss Estimation Methodology, n.d.

[41] Dodaran MV. Impact of adjacent buildings during seismic loads, University of Mohaghegh Ardabili. 1393.

[42] SeismoStruct v7.0 – A computer program for static and dynamic nonlinear analysis of framed structures," available from http://www.seismosoft.com. n.d.

[43] http://ngawest2.berkeley.edu. PEER Ground Motion Database n.d.